analytical chemistry

Article

pubs.acs.org/ac

Surface-Induced Protein Unfolding in Submicron Electrospray Emitters

Daniel N. Mortensen and Evan R. Williams*

Department of Chemistry, University of California, Berkeley, California 94720-1460, United States

Supporting Information

ABSTRACT: The charging of protein ions formed by nanoelectrospray ionization (nanoESI) with tips that are between 1.5 μm and 250 nm in outer diameter is compared. More charging is obtained with the smaller tip sizes for proteins that have a net positive charge in solution, and additional high-charge-state distributions are often observed. A single charge-state distribution of holo-myoglobin ions is produced by nanoESI from a slightly acidified aqueous solution with the micron outer diameter tips, but some apo-myoglobin ions are produced with the submicron tips. In contrast, the charge-state distributions for proteins with a net negative charge in solution do not depend on tip size. Both the formation of high charge states and the appearance of higher-charge-state distributions, as well as the loss of the heme group from myoglobin, indicate that a fraction of the protein population is unfolding with the smaller tips. The increased charging with the smaller tip sizes for proteins with a net positive charge but not for proteins with a net negative charge indicates that the unfolding occurs prior to nanoelectrospray ionization as a result of Coulombic attraction between positively charged protein molecules in solution and the glass surfaces of the emitter tips that are negatively charged. These results demonstrate a novel method for producing highly charged protein ions that does not require exposing the proteins to additional chemicals either in solution or in the gas phase.

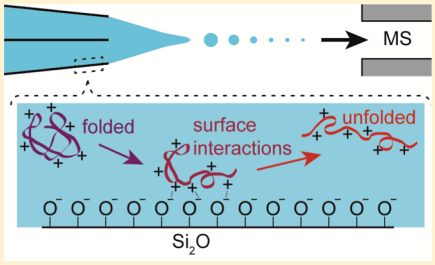

Electrospray ionization (ESI) mass spectrometry (MS) is widely used to identify proteins and to identify posttranslational modifications.[1−3] The charge-state distributions produced by ESI can be used to obtain information about protein conformation. Ions formed by ESI from solutions in which proteins have folded globular structures are less highly charged than those formed from solutions in which proteins are unfolded.[4,5] The charge-state distributions resulting from different protein conformers can be modeled in order to determine the relative abundances of these conformers in solution.[4,6] Other factors that affect the extent of charging in ESI include the solution pH and protein isoelectric point (pI),[7] the solution surface tension,[8,9] the solvent and analyte basicities,[10−12] and instrumental parameters.[13,14]

High-charge-state ions produced by ESI are advantageous because they can be detected more readily on charge detection mass spectrometers, such as FTMS instruments,[15,16] and they are more readily fragmented in tandem MS, often enabling more structural information to be obtained.[17−19] High-charge-state protein ions can be obtained by adding supercharging reagents to solutions in which proteins have either denatured[8,20−26] or native[9,26−32] structures. Higher charge states can also be obtained in native MS by adding trivalent metal ions to analyte solutions prior to ESI,[33] by exposing ESI droplets to either acidic[34] or basic[35] vapors in the MS interface, and by using electrothermal supercharging.[36−38] In electrothermal supercharging, high spray potentials are used to form protein ions from buffered aqueous solutions. These high spray potentials result in collisional heating of the ESI droplets and thermal denaturation of the protein inside the ESI droplet.[36,38]

Increased charging has also been reported for protein and peptide ions when the outer diameter (o.d.) of the tips of the ESI emitters is reduced. The average charge of angiotensin I ions formed from a denaturing solution increased from ∼1.7 to ∼2.8 when the tip o.d. was decreased from ∼5 to ∼1 μm.[39] Higher charge states and narrower charge-state distributions of cytochrome *c* and ubiquitin ions were formed from acidified denaturing solutions with <100 nm o.d. tips than with ∼1 μm o.d. tips.[40] The increased charging obtained with the smaller tip sizes was attributed to smaller droplets with higher charge densities being formed from the smaller tips.[39,40] Electrospray emitters with adjustable orifice sizes have also been reported.[41,42] The horizontal gap width was varied between 1 and >10 μm by adjusting the positions of two triangular-shaped silicon chips. The signal-to-noise ratio and the extent of charging increased with decreasing orifice size for angiotensin I[42] and insulin chain B[41] ions formed from acidified denaturing solutions.

Recently, increased charging and narrower charge-state distributions with decreased tip o.d. were reported for apo-myoglobin and Trp-cage ions formed from acidified aqueous solutions using theta-glass emitters (double-barrel wire-in-a-capillary emitters) with ∼1500 to ∼250 nm o.d. tips.[43] Bimodal charging was also reported for apo-myoglobin ions with the smaller tips, consistent with a fraction of the protein population

Received: June 29, 2016
Accepted: September 12, 2016
Published: September 12, 2016

DOI: 10.1021/acs.analchem.6b02499
Anal. Chem. 2016, 88, 9662−9668

adopting a highly unfolded structure.[43] The formation of this highly unfolded conformer was attributed to protein molecules in solution interacting with the surface of the tips of the emitters prior to nanoESI.[43] The relative abundance of this highly unfolded conformer was constant with spray potential between 450 and 1050 V, indicating that this conformer was not formed as a result of the higher electric field obtained with the smaller tip size.[43] However, in combination with electrothermal supercharging using buffers, emitters with submicron tips result in enhanced supercharging at high spray potentials for proteins with a net positive charge but not for those with a net negative charge in solution.[44] This effect was attributed to destabilizing protein−surface interactions between proteins with a net positive charge and the surfaces of the emitter tips that are negatively charged.

Nano-ESI emitters are generally prepared from borosilicate glass capillaries[39,40,43] or other types of silicon[41,42] which contain silanol groups at the surface.[45] In aqueous solutions, a fraction of the silanol groups is deprotonated, resulting in a negative charge on the glass surface that depends on the pH of the solution.[45] Interactions between positively charged proteins in solution and negatively charged glass surfaces have also been reported to affect the transport times of protein molecules through 5 to 96 nm diameter nanochannels in silica membranes.[46−49] The transport time through the pores depends on the charge of the molecules and on the charge density at the surface of the nanochannels.[49]

Here, theta-glass emitters prepared from borosilicate glass with between ∼1.5 μm and ∼250 nm o.d. tips are used to form protein ions from aqueous solutions using nanoESI. With the submicron o.d. tips, distributions of highly charged ions are formed for proteins with a net positive charge in solution but not for proteins with a net negative charge in solution. These results indicate that Coulombic attraction between the proteins with a net positive charge and the glass surfaces in the small tips of these emitters that are negatively charged results in unfolding of a fraction of the protein population prior to nanoESI. These results show another way to produce highly charged ions that does not require the addition of other chemicals either to the analyte solution or in the gas phase.

EXPERIMENTAL SECTION

Mass spectra were acquired using a 9.4 T Fourier-transform ion cyclotron resonance mass spectrometer, which is described in detail elsewhere.[50] Protein ions are formed by nanoelectrospray ionization using theta glass capillaries (Warner Instruments, LLC, Hamden, CT) with tips that are pulled using a model p-87 Flaming/Brown micropipette puller (Sutter Instruments Co., Novato, CA). Electron micrographs of the tips of the emitters mounted on carbon tape (Figure 1) are obtained at a magnification of 10 000-times using a TM-1000 scanning electron microscope (Hitachi High-Technologies Co., Tokyo, Japan). Grounded platinum wires are brought into contact with the solutions in the emitters, and nanoESI is initiated by applying about a −700 V potential to the heated capillary of the ESI interface. Data are acquired with a Predator data station,[51] and the mass spectra are background subtracted. Average charge is computed as an abundance weighted sum of the individual charge states. Uncertainties are reported as standard deviations determined from three replicate experiments.

Ammonium acetate, equine apo- and holo-myoglobin, equine cytochrome *c*, and bovine β-lactoglobulin A are obtained from Sigma-Aldrich (St. Louis, MO), and glacial acetic acid is from Fisher Scientific (Fair Lawn, NJ). Solutions have a 10 μM analyte concentration and are prepared in 18.2 MΩ water from a Milli-Q water purification system (Millipore, Billerica, MA).

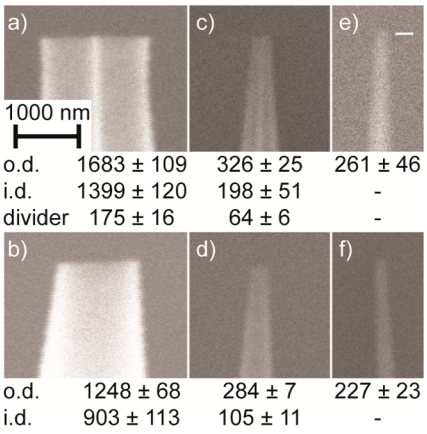

Figure 1. Electron micrographs of the tips of the theta-glass emitters with average outer diameters of (a,b) 1465 ± 134, (c,d) 305 ± 32, and (e,f) 244 ± 61 nm with the inner divider perpendicular to and parallel to the sample stand in the upper and lower panels, respectively. A white line was added to (e) to indicate where the tip ends.

RESULTS AND DISCUSSION

Charging of Apo-Myoglobin and Tip Size. Mass spectra of an acidified aqueous aMb solution (pH = 2.9) obtained using theta-glass emitters with 1465 ± 134, 305 ± 32, and 244 ± 61 nm o.d. tips are shown in Figure 2a−c, respectively. Apo-

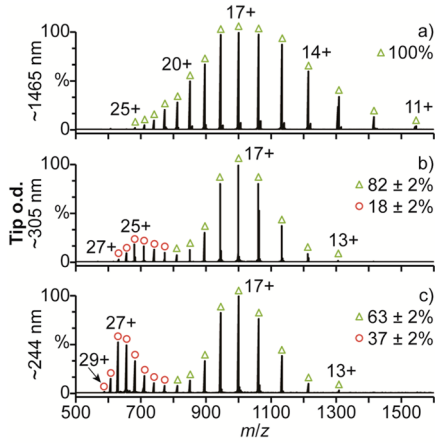

Figure 2. Mass spectra of aMb in an acidified aqueous solution (pH = 2.9) acquired with theta-glass emitters with (a) ∼1465, (b) ∼305, and (c) ∼244 nm o.d. tips.

myoglobin (aMb) adopts a globular conformation similar to the native conformation of holo-myoglobin in aqueous solutions between pH = 5 and 7, a less-compact globular conformation at pH = 4, and a partially unfolded conformation below pH = 3.[52] A single charge-state distribution center at 17+ is formed with the ∼1465 nm o.d. tips (Figure 2a). The breadth and position of this distribution is consistent with aMb adopting a range of unfolded structures in this solution. The charge-state distribution is bimodal with the smaller ∼305 nm o.d. tips (Figure 2b), with one distribution centered at 17+, corresponding to partially unfolded conformers and comprising 82 ± 2% of aMb, and another distribution centered at 25+,

DOI: 10.1021/acs.analchem.6b02499
Anal. Chem. 2016, 88, 9662−9668

comprising 18 ± 2%. The distribution centered at 25+ is consistent with the formation of a distribution of more highly unfolded conformers. With the even smaller ~244 nm o.d. tips (Figure 2c), the relative abundance and maximum charge state of the highly unfolded conformers increase to 37 ± 2% and to the 29+ charge state, respectively. The surface area relative to the solution volume in the nanoESI-emitter tips increases as the tip size decreases, and the surfaces in these tips likely cause changes to the protein structure for a fraction of the population prior to nanoESI.

To compare the charging obtained with single-barrel emitters and theta-glass emitters, single-barrel borosilicate emitters with 1448 ± 135 and 269 ± 29 nm o.d. tips were prepared (Figure 3a,b, respectively). In the mass spectra of aMb in acidified

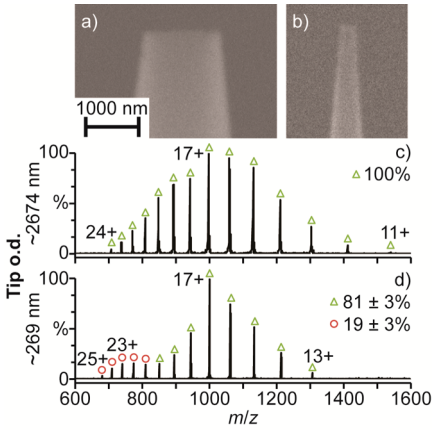

Figure 3. Electron micrographs of the tips of the single-barrel emitters with average outer diameters of (a) 1448 ± 135 and (b) 269 ± 29 nm. Mass spectra of aMb in an acidified aqueous solution (pH = 2.9) acquired with single-barrel emitters with (c) ~ 2674 and (d) ~ 269 nm o.d. tips.

solution (pH = 2.9) obtained with the 1448 ± 135 nm o.d. tips (Figure 3c), only a single charge-state distribution centered at 17+ is observed. This distribution is consistent with aMb adopting a range of unfolded conformers in this solution and is very similar to the charge-state distribution centered at 17+ obtained with the ~1465 nm o.d. tip theta-glass emitters (Figure 2a). With the 269 ± 29 nm o.d. tips (Figure 3d), the charge-state distribution is bimodal, with distributions centered at 17+ and 23+, comprising 81 ± 3% and 19 ± 3% of aMb, respectively. These charge-state distributions are consistent with partially and highly unfolded conformers, respectively. The relative abundance of the highly unfolded conformers obtained with the single-barrel emitters with 269 ± 29 nm o.d. tips (19 ± 3%, Figure 3d) is less than that obtained with the theta-glass emitters with the ~244 nm o.d. tips (37 ± 2%, Figure 2c). The greater extent of highly unfolded conformers obtained with the theta-glass emitters is likely due to the central divider resulting in a greater surface area in the tips of these emitters compared to that in the tips of single-barrel emitters with similar tip sizes.

Charging of Cytochrome *c* and Tip Size. To determine if high-charge-state distributions of other proteins can also be produced with the smaller tip sizes, similar experiments were performed with cytochrome *c* (cyt *c*). In aqueous solutions containing <0.2 M salt concentrations, cyt *c* adopts a native globular conformation between pH = 3 and 7 and a partially unfolded conformation at pH = 2.[53,54] Between pH = 2 and 3, the folded and partially unfolded structures exist in equilibrium.[54] Mass spectra of an acidified aqueous cyt *c* solution (pH = 2.8) obtained using theta-glass emitters with ~1465, ~ 305, and ~244 nm o.d. tips are shown in Figure 4a–

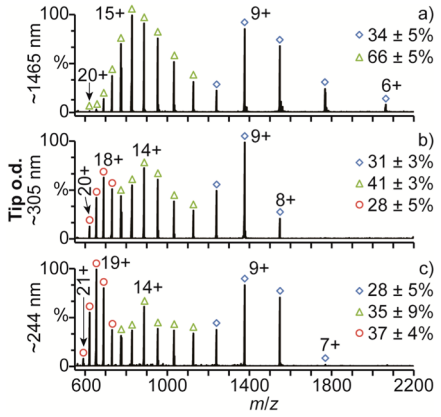

Figure 4. Mass spectra of cyt *c* in an acidified aqueous solution (pH = 2.8) acquired with (a) ~ 1465, (b) ~ 305, and (c) ~ 244 nm o.d. tips.

c, respectively. The charge-state distribution is bimodal with the ~1465 nm o.d. tips (Figure 4a), with charge-state distributions centered at 9+ and 15+, comprising 34 ± 5% and 66 ± 5% of the population, respectively. These distributions are consistent with folded and partially unfolded structures, respectively. With the smaller ~305 nm o.d. tips (Figure 4b), charge-state distributions centered at 9+ and 14+ are observed, comprising 31 ± 3% and 41 ± 3% of cyt *c*, respectively. These distributions are similar to those obtained with the larger ~1465 nm o.d. tips (Figure 4a) and are consistent with folded and partially unfolded conformers, respectively. In addition, a third distribution centered at 18+ is formed, comprising 28 ± 5% of the population. This third distribution is consistent with the formation of more highly unfolded cyt *c* conformers. With the smallest ~244 nm o.d. tips (Figure 4c), the relative abundance and maximum charge state of the highly unfolded conformers increase to 37 ± 4% and to the 21+ charge state, respectively.

The relative abundance of the folded cyt *c* conformer decreases by only ~6% when the tip o.d. is reduced from ~1465 nm (34 ± 5%, Figure 4a) to ~244 nm (28 ± 5%, Figure 4c), but the relative abundance of the partially unfolded conformers decreases by ~31% with this reduction in tip size (66 ± 5% and 35 ± 9% in Figure 4a,c, respectively). These results indicate that the population of highly unfolded conformers is formed predominantly from the partially unfolded conformers and that only a small fraction of the folded conformer is unfolded by the surfaces in these experiments. Partially unfolded proteins may interact more strongly with the glass surfaces than fully folded proteins because of their greater surface areas, which may result in even more unfolding. The transition from a folded form to an unfolded form may also have a higher activation barrier compared to the transition from a partially unfolded form to a highly unfolded form of the population.

The charge-state distribution corresponding to partially unfolded structures is centered at 15+ with the ~1465 nm o.d. tips (Figure 4a) and at 14+ with the smaller ~305 and ~244 nm o.d. tips (Figure 4b,c, respectively). This shift to lower charge with decreasing tip size may suggest that the broad charge-state distribution obtained for the partially unfolded conformers with the larger ~1465 nm o.d. tips is

DOI: 10.1021/acs.analchem.6b02499
Anal. Chem. 2016, 88, 9662–9668

composed of unresolved charge-state distributions resulting from a distribution of partially unfolded conformers. The partially unfolded conformers that result in higher charging with the larger tips likely unfold more readily with the smaller tips, resulting in a shift in the partially folded distribution in Figure 4b to slightly lower charge. These results suggest that more information about the number of solution-phase protein conformers can be obtained with multiple tip sizes than with a single tip size.

Mechanism of Increased Charging with Decreasing Tip Size. To confirm that the high charge-state distributions obtained with the submicron o.d. tips result from protein unfolding, experiments were performed with holo-myoglobin (hMb). In aqueous solutions, hMb adopts a native globular conformation between pH = 5 and 7,[55] a less-compact globular conformation around pH = 3,[55] and a partially unfolded conformation without the heme group attached at lower pH.[56] NanoESI of hMb in a slightly acidified aqueous solution (pH = 4.1) with a ~ 1465 nm o.d. tip (Figure 5a) results in the 7−12+

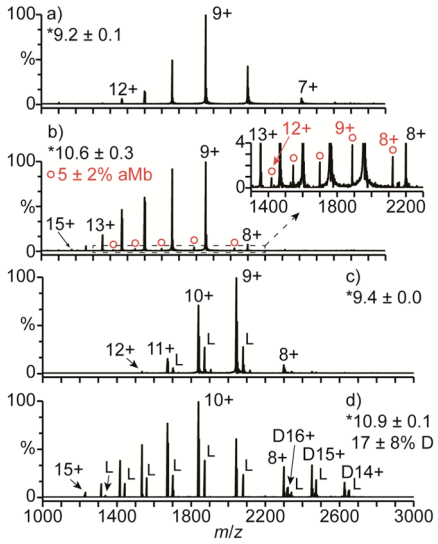

Figure 5. Mass spectra of (a,b) hMb and (c,d) β-lac A in slightly acidified aqueous solutions (pH = 4.1) acquired with (a,c) ~ 1465 and (b,d) ~ 305 nm o.d. tips. (*) denotes average charge. (L) denotes β-lac A with a covalently bound lactosyl molecule.[58,69] (D) denotes dimers.

charge states with an average charge of 9.2 ± 0.1, consistent with hMb adopting folded conformations in this solution. With smaller ~305 nm o.d. tips (Figure 5b), the average charge of hMb increases to 10.6 ± 0.3 and the 8−12+ charge states of aMb are formed, comprising 5 ± 2% of myoglobin. Some structural changes to hMb must occur in order for loss of the heme to occur with the smaller tips. The presence of aMb, which is formed by loss of the heme group from hMb, indicates that a fraction of myoglobin is partially unfolded with the ~305 nm o.d. tips. Both the higher charging and the loss of heme that occur with the smaller tips indicate that the smaller tips induce a structural change in the protein. The similar distributions of charge states for hMb and aMb suggest that the formation of higher charge states and the loss of heme are related. These results also indicate that extensive unfolding of the protein does not occur.

Results with β-lactoglobulin A (β-lac A), which aggregates upon denaturation,[57,58] provide additional support for increased charging at small tip size resulting from protein unfolding. Mass spectra of β-lac A in a slightly acidified aqueous solution (pH = 4.1) obtained with ~1465 and ~305 nm o.d. tips are shown in Figure 5c,d, respectively. The 8−12+ charge states of β-lac A are formed with the larger ~1465 nm o.d. tips (Figure 5c), and the average charge is 9.4 ± 0.0. With the smaller ~305 nm o.d. tips (Figure 5d), the average charge is 10.9 ± 0.1 (8−15+ charge states), and the 14−16+ charge states of β-lac A dimers are formed, comprising 17 ± 8% of the population. The formation of these dimers likely results from the aggregation of unfolded monomers, consistent with protein unfolding occurring with the smaller tips.

Both myoglobin (pI = 7.4)[59] and cyt *c* (pI = 10.3)[60] have net positive charge in the pH ≤ 4.1 solutions used to obtain the data in Figures 2−5. The nanoESI emitters are borosilicate glass, which has a surface that is negatively charged in these aqueous solutions.[45] Coulombic attraction between proteins with a net positive charge in solution and the glass surfaces in the nanoESI-emitter tips that are negatively charged likely leads to protein−surface interactions that destabilize protein structure, an effect that should be more pronounced with smaller tip sizes owing to the higher surface-to-volume ratios. To provide evidence for this mechanism, results are obtained from buffered aqueous solutions with pH values both above and below the pI = 7.4 of hMb. In a 100 mM aqueous ammonium acetate solution (pH = 6.7), hMb has a net positive charge. NanoESI of this solution with a ~1465 nm o.d. tip (Figure 6a) results in the 7−9+ charge states with an average

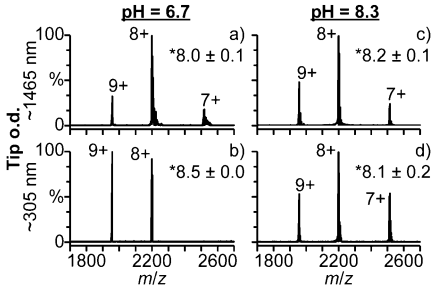

Figure 6. Mass spectra of hMb (pI = 7.4) in aqueous solutions containing (a,b) 100 mM ammonium acetate (pH = 6.7) and (c,d) 100 mM ammonium bicarbonate (pH = 8.3) acquired with (a,c) ~1465 and (b,d) ~305 nm o.d. tips. (*) denotes average charge.

charge of 8.0 ± 0.1, consistent with hMb adopting a folded native-like structure in solution. With a smaller ~305 nm o.d. tip (Figure 6b), there is no 7+ charge state and the average charge is shifted higher to 8.5 ± 0.0, consistent with a change to a slightly unfolded protein structure occurring with the smaller tips.

In a 100 mM aqueous ammonium bicarbonate solution (pH = 8.3), hMb has a net negative charge. Results obtained for this solution with ~1465 and ~305 nm o.d. tips are shown in Figure 6c,d, respectively. The 7−9+ charge states are formed and the average charge is the same to within error for each tip size (8.2 ± 0.1 and 8.1 ± 0.2 in Figure 6c,d, respectively). These results are nearly identical to those obtained for the ammonium acetate solution with the larger tip size (Figure 6a) and are consistent with hMb adopting a folded native-like structure in solution. These results indicate that reducing the tip o.d. within this range of tip sizes does not result in a measurable change to the protein structure when the solution pH (8.3) is greater than the protein pI (7.4). The stability of

DOI: 10.1021/acs.analchem.6b02499
Anal. Chem. 2016, 88, 9662−9668

the folded hMb conformer in aqueous ammonium bicarbonate solutions is the same as that in aqueous ammonium acetate solutions with similar buffer concentrations.[37] Thus, the effects of tip size on the charge state distribution at pH = 6.7 but not at pH = 8.3 is not due to a difference in protein stability in these solutions. These results are consistent with the increased charging and protein unfolding obtained by decreasing the tip o.d. resulting from Coulombic attraction between proteins with a net positive charge in solution and the glass surfaces in the nanoESI-emitter tips that are negatively charged. These results are also consistent with the increased charging resulting from electrothermal supercharging obtained with decreasing tip size for proteins with a net positive charge but not for proteins with a net negative charge in solution.[44]

Effects of ionic strength on the increased charging at small tip size was investigated. Mass spectra of hMb with the ∼1465 and ∼305 nm o.d. tips were acquired from 10, 100, and 500 mM aqueous ammonium acetate solutions in which hMb has a net positive charge. The average charge is 8.0 ± 0.1 for each ammonium acetate solution with the ∼1465 nm o.d. tips (Supporting Information, Figure S-1a−c, respectively). With the ∼305 nm o.d. tips, the average charge is 8.5 ± 0.0, 8.5 ± 0.0 and 8.3 ± 0.1 for the 10, 100, and 500 mM ammonium acetate solutions, respectively (Figure S-1d−f). The slightly lower average charge with the 500 mM solution may be due to increased ammonium−surface interactions in the tips of the emitters. Ammonium−surface interactions could lower the effective net charge on the surface of the emitters,[61] which could result in less unfolding occurring prior to nanoESI. The higher ammonium acetate concentration may also increase the stability of the folded conformation, resulting in fewer conformational changes occurring. Spectra were also acquired from 10, 100, and 500 mM aqueous ammonium bicarbonate solutions in which hMb has a net negative charge (Supporting Information, Figure S-2). The average charge of hMb ions is the same to within error at each concentration and with both tip sizes, consistent with no destabilizing interactions between the negatively charged proteins and tip surfaces occurring.

Support for protein unfolding as a result of Coulombic attraction between the proteins and the glass surfaces is also obtained using 100 mM aqueous ammonium acetate solutions (pH = 6.7) containing either negatively or positively charged proteins. β-lac A (pI = 5.1)[62] has a net negative charge in aqueous solutions at pH = 6.7. Results for β-lac A in the ammonium acetate solution obtained with ∼1465 and ∼305 nm o.d. tips are shown in Figure 7a,b, respectively. The 7−9+ charge states are formed and the average charge is the same at each tip size (8.0 ± 0.3 and 8.0 ± 0.2 in Figure 7a,b, respectively). β-lac A has a globular native structure between pH = 2.0 and 6.2 and is slightly unfolded at pH = 7.5.[63] The results in Figure 7a,b are consistent with β-lac A adopting a folded conformation in solution. The similar results obtained with the different tip sizes indicate that reducing the tip o.d. from ∼1465 to ∼305 nm does not result in measurable unfolding occurring for β-lac A in this solution.

Cyt *c* (pI = 10.3)[60] has a net positive charge in aqueous solutions at pH = 6.7. Results obtained for cyt *c* in a 100 mM aqueous ammonium acetate solution with ∼1465 and ∼305 nm o.d. tips are shown in Figure 7c,d, respectively. The 6−8+ charge states are formed with the ∼1465 nm o.d. tips (Figure 7c), consistent with cyt *c* adopting a folded conformation in solution. Charge states corresponding to both folded (6−8+) and unfolded (9−13+) conformers are formed with the smaller

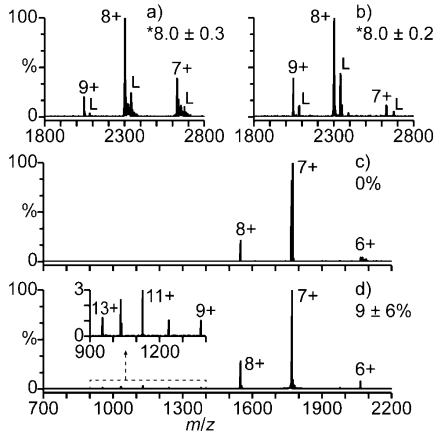

Figure 7. Mass spectra of (a,b) β-lac A (pI = 5.1) and (c,d) cyt *c* (pI = 10.3) in 100 mM aqueous ammonium acetate solutions (pH = 6.7) acquired with (a,c) ∼ 1465 and (b,d) ∼ 305 nm o.d. tips. (*) denotes average charge. (L) denotes β-lac A with a covalently bound lactosyl molecule.[58,69] Percentages are the relative abundances of the unfolded fractions (9−13+ charge states) of cyt *c*.

∼305 nm o.d. tips (Figure 7d), and the unfolded conformers comprise 9 ± 6% of the population. The formation of ions corresponding to unfolded cyt *c* with the ∼305 nm o.d. tips is consistent with the positively charged cyt *c* molecules interacting with the glass surfaces in the smaller tips of these emitters that are negatively charged.

Comparison with Previous Results. Higher charging with smaller tip sizes has been previously attributed to smaller droplets with higher charge densities being formed with decreasing tip size.[39,40] However, the results from those studies are also consistent with surface-induced unfolding in the tips of the emitters. For example, nanoESI mass spectra of cyt *c* in a denaturing solution obtained with ∼1 μm and 58 nm o.d. tips were reported.[40] The mass spectrum obtained with the larger ∼1 μm o.d. tip shows a single charge-state distribution centered at 15+, whereas there is a bimodal charge-state distribution centered at 11+ and 17+ with the smaller 58 nm o.d. tip. The formation of highly charged droplets with the smaller tip size would not likely result in the formation of a distribution centered at a lower charge state (11+) than that obtained with the larger tip size (15+), nor would a bimodal charge-state distribution be expected. It is likely that the distribution centered at 15+ with the ∼1 μm o.d. tip corresponds to a distribution of partially unfolded conformers. The distribution centered at 17+ obtained with the 58 nm o.d. tip may correspond to highly unfolded structures resulting from surface-induced unfolding in the tip of the emitter, which shift the other distribution lower to 11+ due to partially unfolded conformers that are not substantially unfolded by the surface in the tip of the emitter.

It is interesting to note the differences in the results obtained for cyt *c* in a denaturing solution in the previous study to those obtained here with the 1% aqueous acetic acid solution (Figure 4). A bimodal charge-state distribution is obtained here with the micron o.d. tips, whereas a highly charged single distribution was reported with a micron o.d. tip previously,[40] indicating that the solution used here is less denaturing than that used previously. However, the charge-state distribution obtained here for the highly unfolded conformers with the ∼244 nm o.d. tips (Figure 4c) is centered at a higher charge state (19+) and has a higher maximum charge state (21+) than

DOI: 10.1021/acs.analchem.6b02499
Anal. Chem. 2016, 88, 9662−9668

that obtained previously with the more denaturing solution and an even smaller 58 nm o.d. tip (high charge state distribution centered at 17+ with a maximum charge state of 20+).[40] Higher charging is likely obtained here because the surface tension of the 1% aqueous acetic acid solution used here (~65 dyn cm^{-1})[64] is higher than that of the 30/70/0.1 water, methanol, acetic acid solution used previously (~27 dyn cm^{-1}).[65] Preferential evaporation of the more volatile solvents will enrich both solutions in acetic acid, and pure acetic acid has a surface tension of ~27 dyn cm^{-1}.[64] These results indicate that the average surface tension in the droplets formed from the solution used here is higher than the average surface tension in the droplets formed from the solution used previously. Charging in ESI increases with increasing surface tension of the droplets.[8,9]

It was argued previously that the higher charging obtained with smaller tip sizes for protein and peptide ions does not result from conformational changes because this effect was observed for angiotensin I, a 10 residue peptide, and it was assumed that this peptide is too small to have significant secondary structure.[39,66] However, angiotensin I has a solution-phase structure containing a hydrophobic core,[67] and structural transitions have been reported for peptides containing as few as 5 residues.[68] Similar shifts in charge reported for angiotensin I with ~1 and ~5 μm o.d. tips[39] were used to monitor changes to the solution-phase structures of both the 20 residue "mini-protein" Trp-cage and the 14 residue peptide renin substrate tetradecapeptide.[43] These results indicate that the increased charging obtained with decreasing tip size for angiotensin I likely results from surface-induced unfolding in the tips of the emitters.

CONCLUSIONS

The charging of protein ions formed by nanoESI with borosilicate glass capillary emitters that have micron and submicron o.d. tips is compared. High charge states are formed with the submicron o.d. tips for proteins with a net positive charge in solution, and additional high-charge-state distributions are often observed. There is a single charge-state distribution for hMb with the micron o.d. tips that is consistent with a folded hMb structure, but with the submicron o.d. tips, the average charge of the hMb ions increases and some aMb is produced. These results indicate that a fraction of the protein population is partially unfolded with the smaller tips. Higher charging with smaller emitter tips occurs for proteins with a net positive charge in solution but not for proteins with a net negative charge in solution. These results indicate that the increased charging and protein unfolding obtained with the submicron o.d. tips for proteins with a net positive charge in solution results from Coulombic attraction to the glass surfaces in the submicron o.d. tips that are negatively charged. More unfolding occurs for proteins that are partially unfolded than for proteins that are folded. Partially unfolded proteins may interact more with the glass surfaces than folded proteins as a result of their greater surface areas, which may result in even more unfolding. The transition from a folded structure to an unfolded structure may also have a higher activation barrier than the transition from a partially unfolded structure to a highly unfolded structure.

Results from these experiments demonstrate a novel method for producing highly charged protein ions from aqueous solutions that does not require exposing the proteins to additional chemicals, either in solution or in the gas phase. These results also clearly show that investigations into how various factors affect charging of gaseous protein ions formed by ESI, such as addition of supercharging reagents, must take into account the effects of ESI emitter tip size on destabilizing protein conformation in solution prior to droplet formation. Protein–surface interactions may also play a role in the commonly reported phenomenon that more highly charged protein ions are often produced as positive ions rather than negative ions.

ASSOCIATED CONTENT

Supporting Information

The Supporting Information is available free of charge on the ACS Publications website at DOI: 10.1021/acs.analchem.6b02499.

Mass spectra of hMb in aqueous solutions containing 10, 100, and 500 mM ammonium acetate or ammonium bicarbonate obtained with ~1465 and ~305 nm o.d. tips (PDF)

AUTHOR INFORMATION

Corresponding Author

*E-mail: erw@berkeley.edu. Phone: (510) 643-7161.

Notes

The authors declare no competing financial interest.

ACKNOWLEDGMENTS

The authors are grateful to the Robert D. Ogg Electron Microscope Lab at the University of California, Berkeley for use of the Hitachi TM-1000 scanning electron microscope and to the National Institutes of Health for financial support (R01GM097357).

REFERENCES

(1) Kruppa, G.; Schoeniger, J.; Young, M. *Rapid Commun. Mass Spectrom.* **2003**, *17*, 155–162.
(2) Aebersold, R.; Mann, M. *Nature* **2003**, *422*, 198–207.
(3) Pan, J.; Borchers, C. H. *Proteomics* **2013**, *13*, 974–981.
(4) Kaltashov, I.; Eyles, S. *Mass Spectrom. Rev.* **2002**, *21*, 37–71.
(5) Liu, J.; Konermann, L. *J. Am. Soc. Mass Spectrom.* **2009**, *20*, 819–828.
(6) Konermann, L.; Rosell, F. I.; Mauk, A. G.; Douglas, D. J. *Biochemistry* **1997**, *36*, 6448–6454.
(7) Pan, P.; Gunawardena, H. P.; Xia, Y.; McLuckey, S. A. *Anal. Chem.* **2004**, *76*, 1165–1174.
(8) Iavarone, A. T.; Williams, E. R. *J. Am. Chem. Soc.* **2003**, *125*, 2319–2327.
(9) Sterling, H. J.; Cassou, C. A.; Trnka, M. J.; Burlingame, A. L.; Krantz, B. A.; Williams, E. R. *Phys. Chem. Chem. Phys.* **2011**, *13*, 18288–18296.
(10) Loo, R. R. O.; Smith, R. D. *J. Mass Spectrom.* **1995**, *30*, 339–347.
(11) Williams, E. R. *J. Mass Spectrom.* **1996**, *31*, 831–842.
(12) Iavarone, A. T.; Jurchen, J. C.; Williams, E. R. *J. Am. Soc. Mass Spectrom.* **2000**, *11*, 976–985.
(13) Thomson, B. *J. Am. Soc. Mass Spectrom.* **1997**, *8*, 1053–1058.
(14) Page, J. S.; Kelly, R. T.; Tang, K.; Smith, R. D. *J. Am. Soc. Mass Spectrom.* **2007**, *18*, 1582–1590.
(15) Marshall, A. G.; Hendrickson, C. L.; Jackson, G. S. *Mass Spectrom. Rev.* **1998**, *17*, 1–35.
(16) Zubarev, R. A.; Makarov, A. *Anal. Chem.* **2013**, *85*, 5288–5296.
(17) Zubarev, R.; Kelleher, N.; McLafferty, F. *J. Am. Chem. Soc.* **1998**, *120*, 3265–3266.
(18) Iavarone, A. T.; Williams, E. R. *Anal. Chem.* **2003**, *75*, 4525–4533.

DOI: 10.1021/acs.analchem.6b02499
Anal. Chem. 2016, 88, 9662–9668

(19) Madsen, J. A.; Brodbelt, J. S. *J. Am. Soc. Mass Spectrom.* **2009**, *20*, 349−358.
(20) Iavarone, A. T.; Jurchen, J. C.; Williams, E. R. *Anal. Chem.* **2001**, *73*, 1455−1460.
(21) Davies, N. W.; Wiese, M. D.; Brown, S. G. A. *Toxicon* **2004**, *43*, 173−183.
(22) Kjeldsen, F.; Giessing, A. M. B.; Ingrell, C. R.; Jensen, O. N. *Anal. Chem.* **2007**, *79*, 9243−9252.
(23) Valeja, S. G.; Tipton, J. D.; Emmett, M. R.; Marshall, A. G. *Anal. Chem.* **2010**, *82*, 7515−7519.
(24) Miladinovic, S. M.; Fornelli, L.; Lu, Y.; Piech, K. M.; Girault, H. H.; Tsybin, Y. O. *Anal. Chem.* **2012**, *84*, 4647−4651.
(25) Teo, C. A.; Donald, W. A. *Anal. Chem.* **2014**, *86*, 4455−4462.
(26) Going, C. C.; Williams, E. R. *Anal. Chem.* **2015**, *87*, 3973−3980.
(27) Lomeli, S. H.; Yin, S.; Loo, R. R. O.; Loo, J. A. *J. Am. Soc. Mass Spectrom.* **2009**, *20*, 593−596.
(28) Sterling, H. J.; Williams, E. R. *Anal. Chem.* **2010**, *82*, 9050−9057.
(29) Hogan, C. J., Jr.; Loo, R. R. O.; Loo, J. A.; de la Mora, J. F. *Phys. Chem. Chem. Phys.* **2010**, *12*, 13476−13483.
(30) Yin, S.; Loo, J. A. *Int. J. Mass Spectrom.* **2011**, *300*, 118−122.
(31) Sterling, H. J.; Kintzer, A. F.; Feld, G. K.; Cassou, C. A.; Krantz, B. A.; Williams, E. R. *J. Am. Soc. Mass Spectrom.* **2012**, *23*, 191−200.
(32) Metwally, H.; McAllister, R. G.; Popa, V.; Konermann, L. *Anal. Chem.* **2016**, *88*, 5345−5354.
(33) Flick, T. G.; Williams, E. R. *J. Am. Soc. Mass Spectrom.* **2012**, *23*, 1885−1895.
(34) Kharlamova, A.; Prentice, B. M.; Huang, T.; McLuckey, S. A. *Anal. Chem.* **2010**, *82*, 7422−7429.
(35) Kharlamova, A.; McLuckey, S. A. *Anal. Chem.* **2011**, *83*, 431−437.
(36) Sterling, H. J.; Cassou, C. A.; Susa, A. C.; Williams, E. R. *Anal. Chem.* **2012**, *84*, 3795−3801.
(37) Hedges, J. B.; Vahidi, S.; Yue, X.; Konermann, L. *Anal. Chem.* **2013**, *85*, 6469−6476.
(38) Cassou, C. A.; Williams, E. R. *Anal. Chem.* **2014**, *86*, 1640−1647.
(39) Li, Y.; Cole, R. B. *Anal. Chem.* **2003**, *75*, 5739−5746.
(40) Yuill, E. M.; Sa, N.; Ray, S. J.; Hieftje, G. M.; Baker, L. A. *Anal. Chem.* **2013**, *85*, 8498−8502.
(41) Ek, P.; Schonberg, T.; Sjodahl, J.; Jacksen, J.; Vieider, C.; Emmer, A.; Roeraade, J. *J. Mass Spectrom.* **2009**, *44*, 171−181.
(42) Ek, P.; Sjodahl, J.; Roeraade, J. *Rapid Commun. Mass Spectrom.* **2006**, *20*, 3176−3182.
(43) Mortensen, D. N.; Williams, E. R. *J. Am. Chem. Soc.* **2016**, *138*, 3453−3460.
(44) Mortensen, D. N.; Williams, E. R. *Analyst* **2016**, *141*, 5598−5606.
(45) Behrens, S. H.; Grier, D. G. *J. Chem. Phys.* **2001**, *115*, 6716−6721.
(46) Pennathur, S.; Santiago, J. *Anal. Chem.* **2005**, *77*, 6782−6789.
(47) Freedman, K. J.; Jurgens, M.; Prabhu, A.; Ahn, C. W.; Jemth, P.; Edel, J. B.; Kim, M. J. *Anal. Chem.* **2011**, *83*, 5137−5144.
(48) Yusko, E. C.; Johnson, J. M.; Majd, S.; Prangkio, P.; Rollings, R. C.; Li, J.; Yang, J.; Mayer, M. *Nat. Nanotechnol.* **2011**, *6*, 253−260.
(49) Anderson, B. N.; Muthukumar, M.; Meller, A. *ACS Nano* **2013**, *7*, 1408−1414.
(50) Jurchen, J. C.; Williams, E. R. *J. Am. Chem. Soc.* **2003**, *125*, 2817−2826.
(51) Blakney, G. T.; Hendrickson, C. L.; Marshall, A. G. *Int. J. Mass Spectrom.* **2011**, *306*, 246−252.
(52) Goto, Y.; Fink, A. L. *J. Mol. Biol.* **1990**, *214*, 803−805.
(53) Shastry, R. M. C.; Luck, S. D.; Roder, H. *Biophys. J.* **1998**, *74*, 2714−2721.
(54) Konno, T. *Protein Sci.* **1998**, *7*, 975−982.
(55) Sage, J. T.; Morikis, D.; Champion, P. M. *Biochemistry* **1991**, *30*, 1227−1237.
(56) Griko, Y. V.; Privalov, P. L.; Venyaminov, S. Y.; Kutyshenko, V. P. *J. Mol. Biol.* **1988**, *202*, 127−138.
(57) Aymard, P.; Nicolai, T.; Durand, D.; Clark, A. *Macromolecules* **1999**, *32*, 2542−2552.
(58) Bouhallab, S.; Morgan, F.; Henry, G.; Molle, D.; Leonil, J. *J. Agric. Food Chem.* **1999**, *47*, 1489−1494.
(59) Bergers, J. J.; Vingerhoeds, M. H.; Vanbloois, L.; Herron, J. N.; Janssen, L. H. M.; Fischer, M. J. E.; Crommelin, D. J. A. *Biochemistry* **1993**, *32*, 4641−4649.
(60) Hemdan, E. S.; Zhao, Y. J.; Sulkowski, E.; Porath, J. *Proc. Natl. Acad. Sci. U. S. A.* **1989**, *86*, 1811−1815.
(61) Stein, D.; Kruithof, M.; Dekker, C. *Phys. Rev. Lett.* **2004**, *93*, 035901.
(62) Kuroda, Y.; Yukinaga, H.; Kitano, M.; Noguchi, T.; Nemati, M.; Shibukawa, A.; Nakagawa, T.; Matsuzaki, K. *J. Pharm. Biomed. Anal.* **2005**, *37*, 423−428.
(63) Kuwata, K.; Hoshino, M.; Forge, V.; Era, S.; Batt, C. A.; Goto, Y. *Protein Sci.* **1999**, *8*, 2541−2545.
(64) Alvarez, E.; Vazquez, G.; Sanchez-Vilas, M.; Sanjurjo, B.; Navaza, J. *J. Chem. Eng. Data* **1997**, *42*, 957−960.
(65) Vazquez, G.; Alvarez, E.; Navaza, J. M. *J. Chem. Eng. Data* **1995**, *40*, 611−614.
(66) Loo, R. R. O.; Lakshmanan, R.; Loo, J. A. *J. Am. Soc. Mass Spectrom.* **2014**, *25*, 1675−1693.
(67) Spyroulias, G.; Nikolakopoulou, P.; Tzakos, A.; Gerothanassis, I.; Magafa, V.; Manessi-Zoupa, E.; Cordopatis, P. *Eur. J. Biochem.* **2003**, *270*, 2163−2173.
(68) Kubelka, J.; Hofrichter, J.; Eaton, W. *Curr. Opin. Struct. Biol.* **2004**, *14*, 76−88.
(69) Leonil, J.; Molle, D.; Fauquant, J.; Maubois, J. L.; Pearce, R. J.; Bouhallab, S. *J. Dairy Sci.* **1997**, *80*, 2270−2281.

DOI: 10.1021/acs.analchem.6b02499
Anal. Chem. 2016, 88, 9662−9668